energies

Review

Operation Issues and Data-Driven Voltage Control in Agile Power Systems

Ali Feliachi [1,*], Farideh Doost Mohammadi [2] and Hessam Keshtkar Vanashi [2]

1 Lane Department of Computer Science and Electrical Engineering, West Virginia University, Morgantown, WV 26506, USA
2 The Department of Physics, Computer Science and Engineering, Christopher Newport University, Newport News, VA 23606, USA
* Correspondence: alfeliachi@mail.wvu.edu

Abstract: This paper defines an agile power system as a system in which the physical structure can change due to the connection/disconnection of subsystems, such as microgrids. These systems pose serious difficulties in their operations and control. Some of these challenges are reviewed. One operational issue is the energy balancing or the load frequency control problem when microgrids with a low inertia are connected to the main grid. The paper identifies the need for new rules of operation. Furthermore, in this paper, decentralized and data-driven voltage control designs are proposed, compared and illustrated on a microgrid. They take into consideration the structure and the usage of the large amount of data provided by the proliferation of sensors.

Keywords: electric power systems; low inertia systems; load frequency control; data-driven voltage control; microgrids

Citation: Feliachi, A.; Mohammadi, F.D.; Vanashi, H.K. Operation Issues and Data-Driven Voltage Control in Agile Power Systems. *Energies* **2022**, *15*, 8125. https://doi.org/10.3390/en15218125

Academic Editor: Abu-Siada Ahmed

Received: 15 September 2022
Accepted: 26 October 2022
Published: 31 October 2022

1. Introduction

The paper defines an agile power system as a system whose physical structure can change due to the connection/disconnection of subsystems such as microgrids. With the integration of renewable resources into the power system, the flexibility of the grid is defined as the capability of the system to provide the demand [1] by utilizing these resources. These systems face serious difficulties in their operation and control. An overview of these challenges is presented in this paper. The control of such systems is essential for their operation. It needs to take into account or take advantage of the newly available computing and communication technologies. The handling of the physical constraints and the large amount of data available will require novel control design methodologies and rules of operation. Topics that will be of interest in addressing some of these concerns include, but are not limited to:

- Data driven control;
- Artificial Intelligent system control;
- Multi-agent Control;
- Hierarchical and Decentralized Control;
- Control of Interconnected Smart Grids.

There are many challenging control problems, such as low inertia issues [2] and voltage control. These two problems are addressed here.

A flexible or agile system, illustrated in Figure 1, is a system that comprises the main grid to which other subsystems such as microgrids or electric vehicles or storage can "come and go" due to several factors including weather, cyber or physical attacks, resource availability or depletion, or malfunctions. It can be one agile "grid" or multiple islanded smaller grids or microgrids, with the possibility of morphing back into the agile system. The abundant amount of information provided by the communication infrastructure can be utilized to improve the control and operation of these systems.

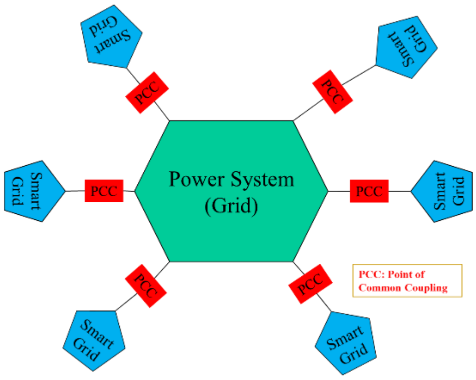

Figure 1. A Schematic of an Agile Power System.

The paper is organized as follows. In Section 2, following this brief introduction, an overview of the challenges facing agile systems is presented. In Section 3, an operation problem that is affected by the interconnection of microgrids with low inertia is the energy balance or the load frequency control problem. The objective of this section is to demonstrate that new rules of operation and interconnection might be needed. In Section 4, the voltage control design in microgrids or other subsystems in the agile system is presented. Both decentralized and data-driven voltage control approaches are proposed that take into consideration the usage of the large amount of data provided by the proliferation of sensors throughout the system due to their decreasing costs.

2. Overview of the Challenges

Future agile power systems face many challenges related to the proliferation of new technologies in computing and communication, the integration of various renewable resources, but also policies and social aspects, including the following:

- Social and Economic Policies;
- Multiple Infrastructures;
- Transportation: Electric Vehicles;
- Information and Communication;
- Data Analytics;
- Data Availability;
- Data Security;
- Integration of Microgrids and Renewable Resources;
- Dispatch;
- Operation Constraints;
- Control Design;
- Low Inertia subsystems and interconnection;
- two-way power flow and faults effects;
- Frequency/Voltage Control;

A brief discussion related to these issues is provided in the following sections.

2.1. Social and Economic Policies

Social and economic policies determine the level of penetration of renewable resources and energy trading and consumption. The acceptance and promotion of green energy and electric vehicles are social decisions that will challenge the operation of the power system. Social and economic policies will determine whether or not consumers will become prosumers, i.e., both producers and consumers of electricity. The rates the consumers will receive for their excess energy as well as their comfort level will be factors in deciding on their participation in demand response. Residential or commercial solar generation will increase when tax incentives are offered. Electric vehicles can be a source of much needed storage. These multiple market, social and engineering challenges will affect the operation and the resiliency of the power system.

2.2. Multiple Infrastructures

Communication and information systems are an integral part of the cyber-physical power system. Other infrastructures such as electric transportation, water, and gas will also interact with the power system's operation and they are adversely affected during blackouts caused by natural disasters. Electric pumps are not functional during these events. Emergency and backup generation, which could represent as much as 15% of the total capacity in the US, is an important resource that is used only when the system is down. It could be utilized during normal or under stress conditions if managed appropriately.

Figure 2 presents a scenario where there is an electric vehicles fleet operator and the traditional system operator who can communicate together for an economic win–win situation. The power system operator minimizes the cost of energy production and the electric vehicle fleet operator can schedule the charging/discharging of the batteries. The problem could have a satisfactory solution for both operators if they exchange price signals. Based on the load forecast, the grid operator selects the generating units that can supply the load at minimum cost, while taking into consideration the available battery storage provided by the electric vehicle fleet operator. The incremental cost, or the price, is passed to the electric fleet operator who schedules its charging and discharging electric vehicles and provides the information to the grid operator. Such an interaction could result in an economical solution for both of them. In the cover of the August 2022 issue of the IEEE Spectrum [3], one can read "How EVs Can Power the Grid". This issue includes an article "A Road Test for Vehicle-to-Grid Tech" that describes the Dutch city of Utrecht which has hundreds of electric-vehicle charging stations. However, today's grid is not designed for this option yet, even though it might be a challenge that may need to be addressed in the near future.

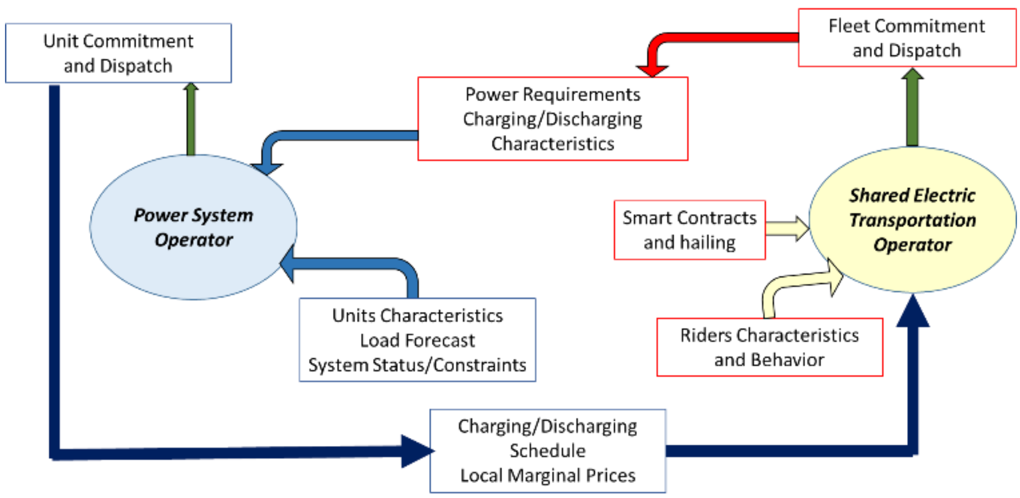

Figure 2. Interaction Between Power System and Electric Fleet Operators.

2.3. Data Analytics

The proliferation of a large number of sensors due to their decreasing cost will result in the collection of an incredibly large amount of data. Additionally, most of the devices are internet ready and allow for communication with other devices, making the system an "Internet of Power Things" [4]. Data analytics and machine learning tools are naturally suited for these scenarios. The difficulties are, however, the unique characteristics of the agile system. Most of these methods require learning with some datasets; however, the system dynamics limit the accuracy of these datasets. Therefore, dedicated computational tools and algorithms are needed.

Smart Contracts, such as the ones based on the blockchain approach, can be utilized for energy trading amongst producers, consumers or storage providers such as electric vehicle riders and the fleet operator, as visible in the scheme depicted in Figure 2. Already, blockchain has been demonstrated to provide a mechanism for consumers and independent producers to buy and sell power. In New York city [5,6], as well as in Denmark, this approach has been implemented for rooftop solar energy trading by neighbors.

Access to this data poses a serious cyber security concern. The grid is faced with daily cyber attacks. The Ukrainian incident [7] of 23 December 2015, is the first of its kind. The information systems of three energy distribution companies were hacked, resulting in temporary disruption in electric power delivery. Securing the system from such events is a difficult task, especially for large agile systems made up of various actors with conflicting objectives. Dedicated cyber protection algorithms are required given the number of vulnerable points of attacks.

2.4. Integration of Microgrids and Renewable Resources

2.4.1. Dispatch

Some of the most attractive and economical renewable resources such as solar and wind energy provide power only intermittently, i.e., only when the sun or the wind are present. Dispatching these units is challenging. Even though there has been an improvement in their forecasting, their output is still considered as a negative load most of the time.

Moreover, such resources are dependent on the availability of the sun and/or wind. Wind farms, for example, are located either offshore or on top of mountains where there exist strong winds. Transporting their power to the load centers might require re-enforcement or the building of new lines, specifically HVDC lines.

2.4.2. Operation Constraints

These intermittent resources will require drastic ramping up or down of the dispatchable units to track the output of the intermittent resources as explained nextterms of traditional units; this is because solar power becomes available at sunrise but disappears at sunset.

Figure 3 is an actual load curve from the California Independent System Operator (CAISO) for 7 October 2022 [8]. The load demand is shown in green and the electricity produced by the traditional units (net demand) is shown in purple. The difference between the green and purple curves is the electricity produced by wind or solar generation. This figure shows a very sharp increase of about 13 GW in 3 h due to the diminishing solar power around sunset.

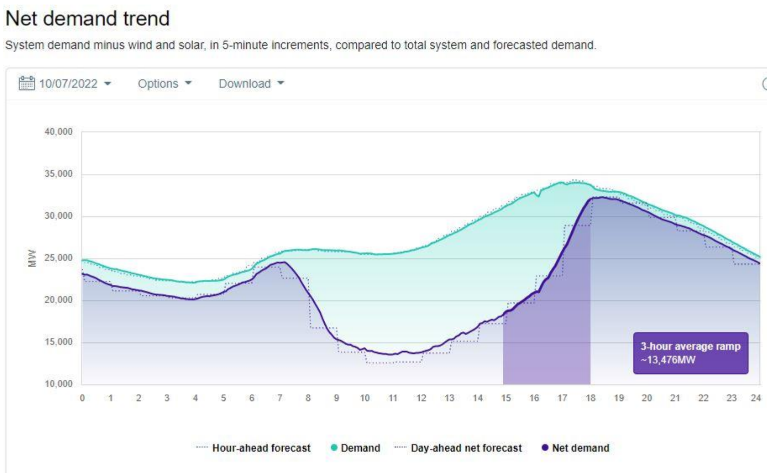

Figure 3. California ISO 10/07/22 Load Curve [8].

2.5. Control Design

The difficulties presented above make the operation and the control of these systems a very challenging problem. Two problems are specifically addressed in the next sections, Sections 3 and 4. They are as follows: (1) the first is related to the low inertia when solving the energy balance or the load frequency control problem, and (2) the second is related to data driven and decentralize voltage control designs, which are presented in Section 4.

3. Effect of Inertia on the Load Frequency Control Problem

The proliferation of inverter-based renewable generation resources, as sketched in Figure 4, results in low-inertia systems. The control and management of the system including stability and load frequency control are challenging [9–14].

Figure 4. Inverter Based Generation [15].

Specifically, for the load frequency control problem the systems analyzed have either two control-areas as shown in Figure 5 or three control-areas. For the two-area system, the areas are classified as Red or Green Areas. These colors are adapted in the figures; red for Area 1 and green for Area 2. The purple color is also used to represent the interchange tie-line power. The tie-line power is a line that connect the control areas and the power flow on this line is preset, based on an agreement between the areas.

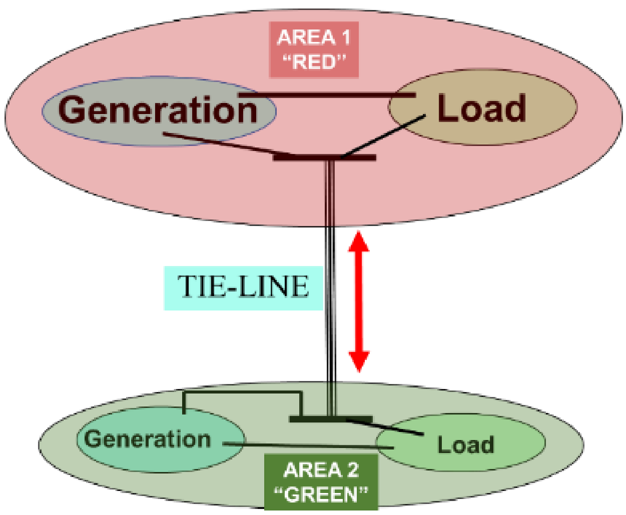

Figure 5. A Two-Area Power System.

A Simulink model of a typical control area is shown in Figure 6.

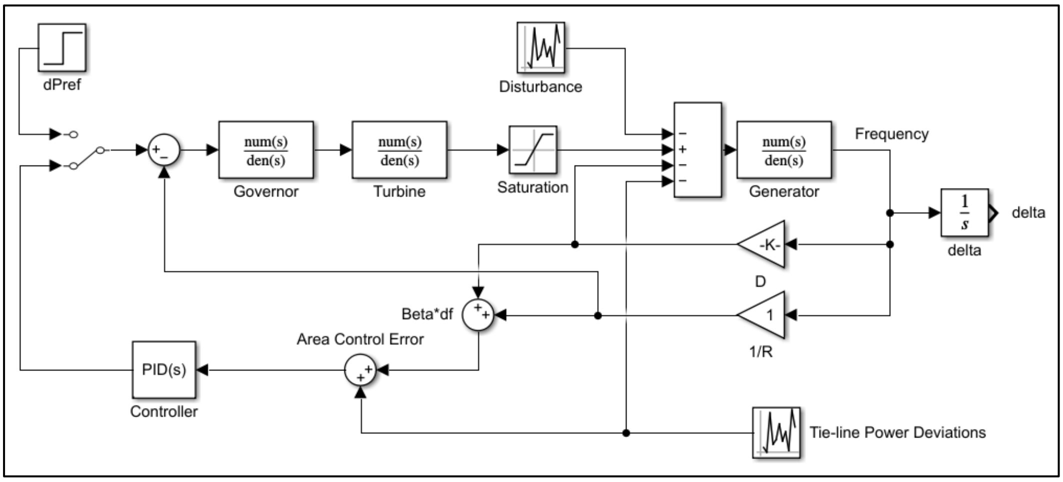

Figure 6. Simulink Model of a Typical Control Area.

Four cases are analyzed to demonstrate the effect of low inertia, each of them with the presence, or a lack of, an area with limited large synchronous generators. In Case 1, Area 1 (Red Area) has a large inertia and Area 2 (Green Area) has a small inertia. In Case 2, both areas have similar inertias. In the second case, the data of Area 3 (Blue Area) in the Table below are used for Area 2. The scenario under study is the effect of a 10% load increase in Area 1. In Cases 3 and 4, a third area (Blue Area) is added. The data used in the simulation are provided in Table 1.

Table 1. System Parameters.

Parameters	Area 1 (Red)	Area 2 (Green)	Area 3 (Blue)
Rating: S_B (MVA), Droop: R (%), R (pu), 1/R	100, 5, 3, 1/3	20, 6, 18, 1/18	75, 4, 3.2, 1/3.2
Common Power Base (MVA)	100	100	100
Constant of Inertia H (seconds), $T_p = 2H/f_0$	4.2, 0.14	3, 0.1	3.9, 0.13
Time Constants: Governor, Turbine (sec)	0.08, 0.4	0.3, 0.6	0.06, 0.4
Damping D (pu MW/Hz)	0.015	0.003	0.014
Synchronizing Power Coefficients (Tie Lines) T_{12}, T_{23}, T_{13}	$T_{12} = 0.015$	$T_{23} = 0.015$	$T_{13} = 0.02$
$\beta = D + 1/R$	0.3483	0.0586	0.3265

Figure 7a shows that the frequency deviations, are unstable in both areas, while the frequency goes back to its nominal value for Case 2, as shown in Figure 7b.

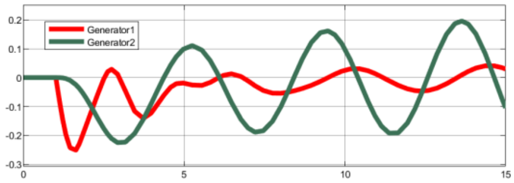

(**a**)

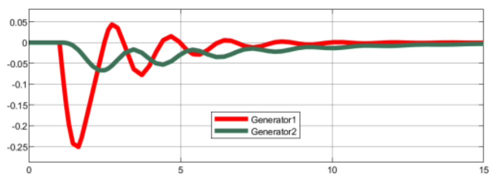

(**b**)

Figure 7. (**a**) Frequency Deviations, Case 1. (**b**) Frequency Deviations, Case 2.

Similarly, the area control errors one and two (ACE 1 and ACE 2) for the two case studies are shown in Figure 8a,b. In Case 1, the area control errors do not return to their pre-fault values, i.e., they do not go back to zero following the disturbance, while in Case 2 the results are as expected and show that the energy balance is restored in both areas.

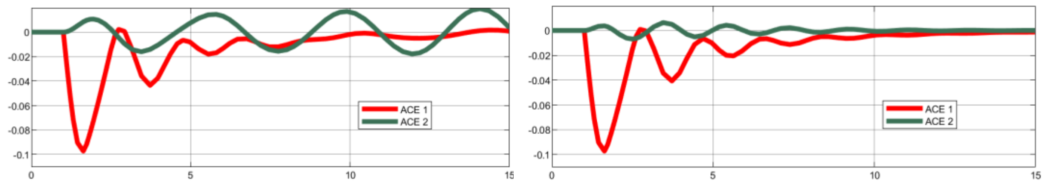

(**a**) (**b**)

Figure 8. (**a**) ACEs (red: ACE 1, green: ACE2), Case 1. (**b**) ACEs (red: ACE 1, green: ACE2), Case 2.

The Area Control Error for area (i) is defined [15] as follows:

$$ACE_i = \sum_j \Delta P_{ij} + \beta_i \Delta f_i \tag{1}$$

where ΔP_{ij} is the deviation from the nominal value of the power flow over the tie-line connecting area i to area j, β_i is a bias or the frequency characteristic of area i, and Δf_i is the deviation from the nominal value of the frequency in area i. To illustrate the issues associated with low inertia, a simple decentralized proportional-integral controller is designed:

$$u_i = k_{pi} ACE_i + k_{ii} \int ACE_i \tag{2}$$

Figure 9 shows the deviation in the power exchange between the areas ΔP_{12}. For Case 1 (Figure 9a), the tie-line power deviation is unstable while for Case 2 (Figure 9b) the tie-line power goes back to its scheduled value.

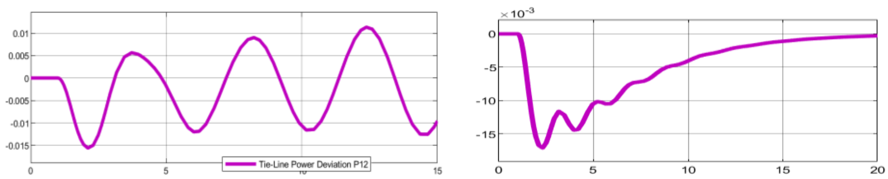

(**a**) (**b**)

Figure 9. (**a**) Tie-Line Power Deviation P12, Case 1. (**b**) Tie-Line Power Deviation: P12, Case 2.

Finally, the incremental mechanical power outputs of both areas are shown in Figure 10. Figure 10a shows that the mechanical power deviations do not reach zero for Case 1, while in Figure 10b the mechanical power deviation in area 2 falls zero since the disturbance is in Area 1.

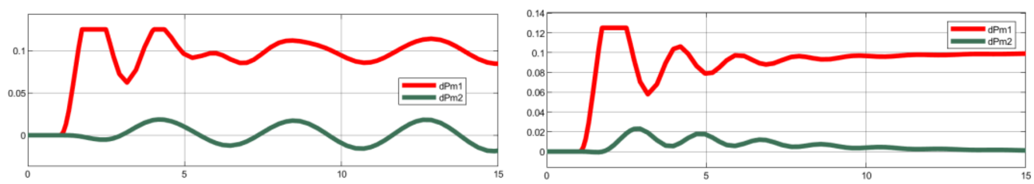

(**a**) (**b**)

Figure 10. (**a**) Mechanical Power Deviation, Case 1. (**b**) Mechanical Power Deviation, Case 2.

The challenge then is to reconsider the expectations when different-sized or inertia systems are interconnected. Traditional measures and expectations for the area frequency errors and control areas statistics need to be revisited, challenging the existing compliance performance measures set by NERC [16]. In this particular case 1 scenario, the solution might be to separate the two areas and each area will be constrained to satisfy its own energy balance. In the case where a microgrid is a DC microgrid, an expensive DC link might be needed to connect it to the system and the frequency control problem will not be an issue.

To analyze this problem further, a third area is added to the previous model using the data provided in Table 1. The following two cases are analyzed: Case 3 uses three areas, Area 1, Area 2 and Area 3 data. Area 2 is the small area. Case 4 uses the three areas, but Area 2 is replaced by the data of Area 3. In Case 3, Area 2 has a small inertia compared to the other two areas. The results obtained are similar to the ones observed for the two-area system. Case 4, where all areas are similar in size, the system is stable; however, Case 3 is unstable. The simulation is performed when a 0.1 pu load increase affects Area 1. Figure 11 shows the frequency deviations in all three areas. In Figure 11a, the frequencies are unstable due to the low inertia area, while in Figure 11b, with all the three areas of comparable inertia, the frequency deviations return to zero. Figures 12–14 show the frequency deviations in all areas, the area control errors, the tie-line power deviations and the mechanical power changes, respectively.

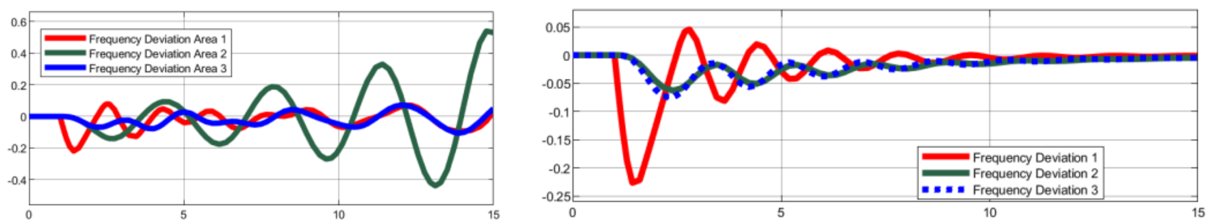

(**a**) (**b**)

Figure 11. (**a**) Frequency Deviations, Case 3. (**b**) Frequency Deviations, Case 4.

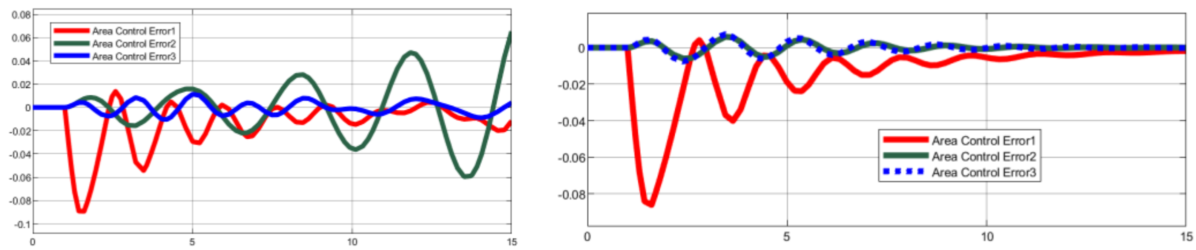

(**a**) (**b**)

Figure 12. (**a**) ACEs, Case 3. (**b**) ACEs, Case 4.

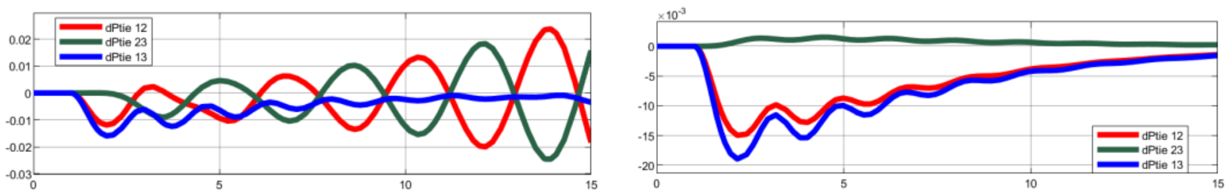

(**a**) (**b**)

Figure 13. (**a**) Tie-Line Power Deviations, Case 3. (**b**) Tie-Line Power Deviations: Case 4.

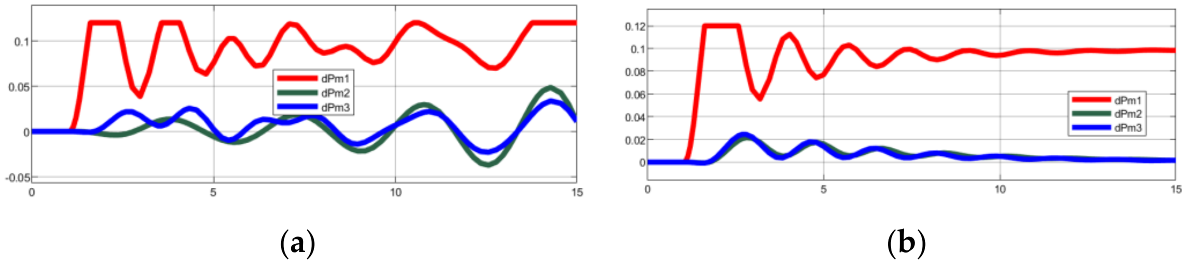

Figure 14. (**a**) Mechanical Power Deviations, Case 3. (**b**) Mechanical Power Deviations, Case 4.

Figure 12 shows the three control-area errors ACE1, ACE2 and ACE3. In Figure 12a, these errors are unstable due to the presence of a low inertia control area, while Figure 12b, with the three areas of comparable size, the three control-area errors return to zero.

Figure 13 shows the tie-line power deviations ΔP_{12}, ΔP_{13}, ΔP_{23}. In Figure 13a, for Case 3, these deviations are unstable, meaning that the power exchanges between areas are increasing. However, in Figure 13b, corresponding to Case 4, the three areas are helping each other during the disturbance by sending power to the area that is in difficulty, which is area 1 that has an increase in power demand. After area 1 has increased its own generation, the tie-line powers return to their scheduled values.

Figure 14 shows mechanical power deviations following the disturbance. This corresponds to the change in generation output in the three areas. In Figure 14a, for Case 3, these deviations are unstable, meaning that the generated power in all three areas is increasing. However, in Figure 14b, corresponding to Case 4, the three areas help each other during the disturbance by generating power and sending it to the distressed area, which is area 1 that faces an increase in power demand. After area 1 has increased its own generation, the other two areas reset their output to their scheduled levels and only Area produces additional power to supply its new demand.

In this section, an issue is raised when operating a system that includes small control areas with small inertias. If these small areas are to be considered as contributors to the load frequency control problem, then the interconnection rules need to reflect these new scenarios.

4. Decentralized and Data-Driven Voltage Controls of Microgrids

The integration of numerous renewable resources to the power system via inverters provides high flexibility along with a complexity in solving the voltage control problem [9]. In this section, decentralized and data-driven-based voltage controllers are developed and compared. It is shown that the performance measures will be improved by incorporating a data-driven-based voltage controller, however, it also leads to the possibility of various types of data failures and cyber-attacks to the infrastructure of the microgrid communication layer [17–19].

For illustration, a data-driven controller (secondary voltage control) is designed for a 12-bus test system, as shown in Figure 15. This system has four inverters connected to buses 1–4, where two of them operate in a Voltage Source Inverter (VSI) mode and the other two are controlled as PQ inverters. Regardless of the chosen secondary voltage control method, the voltage will be controlled by the VSI inverters. In other words, VSI inverters act as the actuators of this control system [10].

In order to discuss the details of the data-driven voltage control method, first, a brief background on the Average Consensus Algorithm (ACA) is provided. Then, the operation of the utilized microgrid with and without the ACA algorithm for the purpose of voltage control is investigated. Finally, the fragilities related to any data-driven control algorithm are discussed. The ACA method, which is implemented as a data-driven approach, is evaluated under some of those weaknesses.

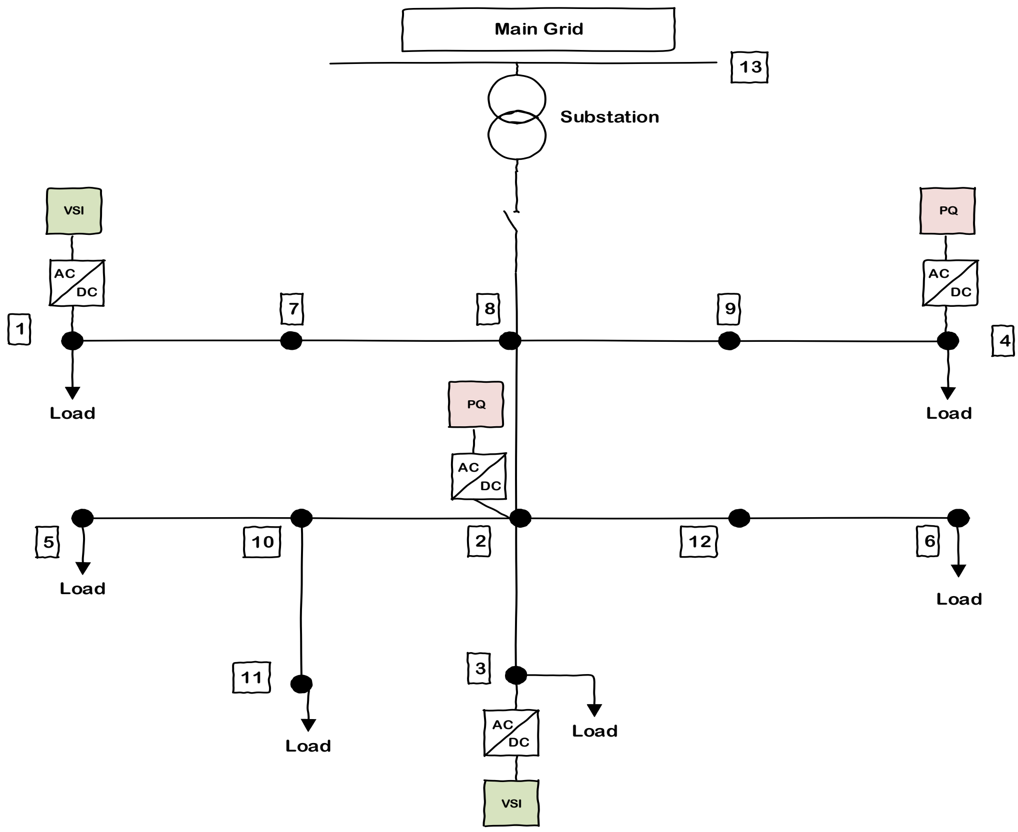

Figure 15. Test System with 12 buses and 4 inverters.

4.1. Background on the Average Consensus Algorithm

In the data-driven voltage control, a multi agent scheme is required where each agent communicates its data to other agents in order to reach a consensus and makes the appropriate control decision. The dynamics of those agents are given in Equation (3) and the applied consensus protocol is described by Equation (4) [20]. In these equations, $u(t)$, $x(t)$, and a_{ij} represent the control input, the state variables, and the components of the updating (adjacency) matrix, A = $[a_{ij}]$, respectively [20]. Figure 16 illustrates the definition of the neighbors of node i and the elements of the adjacency matrix such as a_{ij} and a_{ki}.

$$\dot{x}_i(t) = u_i(t) \tag{3}$$

$$u_i = \sum_{v_j \in N_i} a_{ij}(x_j - x_i) \tag{4}$$

In the average consensus algorithm, reaching an agreement is possible only if the directed graph of agents (also called digraph) is both Balanced and Strongly Connected (SC). A balanced node in a network refers to a node which has equal out-degree and in-degree. If all the nodes included in that network are balanced, the digraph is called balanced. A strongly connected network on the other hand refers to a network in which every node is reachable from every other node through a path with proper direction.

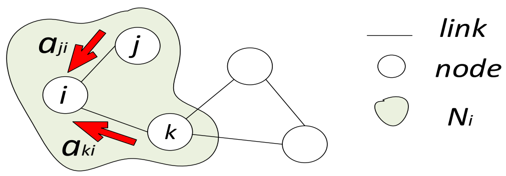

Figure 16. Network Structure of the Communication Layer.

Having a strongly connected digraph ensures an agreement between the agents. However, this group decision value is not necessarily equivalent to the average of the node's initial data. To achieve the average consensus, where the correct average value is the result of the agreement process, the digraph needs to be balanced as well as strongly connected. Here in Figure 17, examples of balanced and unbalanced digraphs are shown.

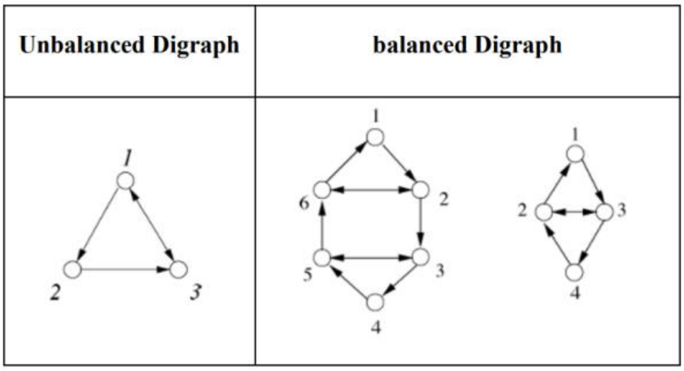

Figure 17. Examples of Balanced and Unbalanced Digraphs.

4.2. Optimum Network Structure and Proper Implementation of the ACA

A data-driven control system uses a network of connected nodes to share data from across the network. The shared data will then be utilized for a consensus agreement problem. To satisfy the required constraint on agreement time delay, specific limits need to be considered while designing the communication network. The first constraint is related to the permissible communication expenses, C_{max}, and the second one is the essential connectivity requirement, K_{min}. In [19], an algorithm is suggested for sketching a digraph with n nodes and the optimum number of edges, contingent on the permissible communication expenses, and the essential connectivity requirements. The outlined diagraph will then demonstrate the connections between the nodes and describe the elements of the adjacency matrix only by ones and zeros (zero refers to no communication link). This procedure is shown in Figure 18, which illustrates the flowchart related to the aforementioned optimum network design.

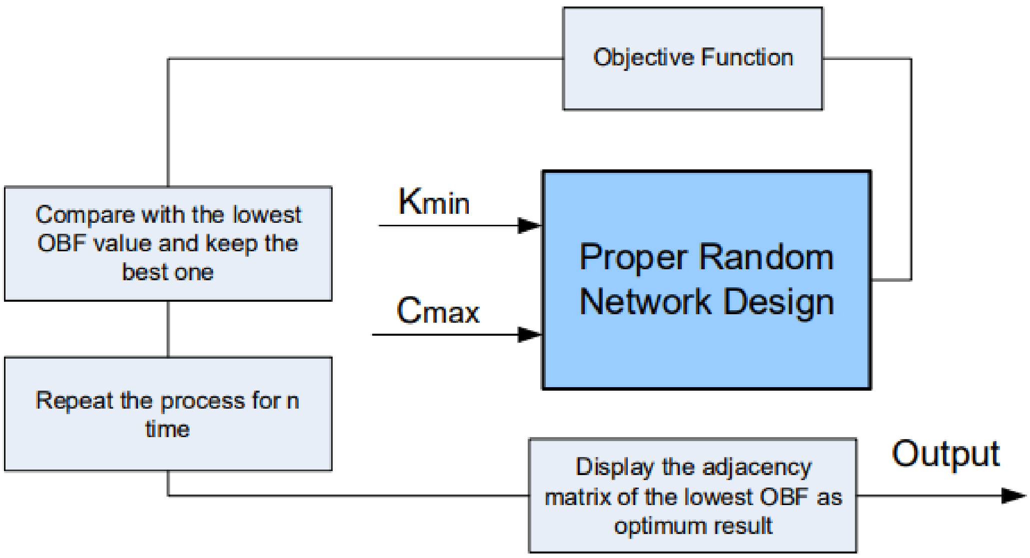

Figure 18. Flowchart for the Optimum Network Design.

The next step for the correct implementation of the ACA would be changing those elements of the adjacency matrix which are equal to one into the required updating weight based on various methods listed as updating protocols [21–23]. The best updating rule is the one which lessens the length of the agreement time delay. It is worth mentioning that the size of the system does not affect the agreement time of the ACA algorithm. The delay is mostly dependent on the graph structure and the selected adjacency matrix. In order to obtain the highest convergence speed, the adjacency matrix is formed by using the Mean Metropolis matrix [21].

Table 2 describes some of the updating rules along with an illustration of their performance. Based on the illustrated performance in this table, the best rule is selected from the table to be used for the understudied microgrid that has twelve buses, with six of them being pilot buses. Then, an optimum network graph with six nodes is adapted for the understudied microgrid which is shown in Figure 19, where the graph is both balanced and strongly connected and therefore capable of reaching consensus.

Table 2. Different Updating Rules Applied on a Graph with 20 Nodes [21].

Updating Rules **(Utilized for a Graph with 20 Nodes in Its Network Layer)**	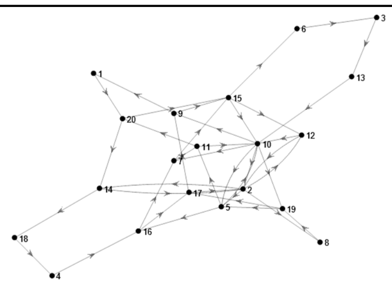
Uniform Weights n: number of nodes	$$a_{ij} = \begin{cases} \frac{1}{n} & j \in N_i \\ 1 - \sum\limits_{j \in N_i} \frac{1}{n} & j = i \\ 0 & otherwise \end{cases}$$
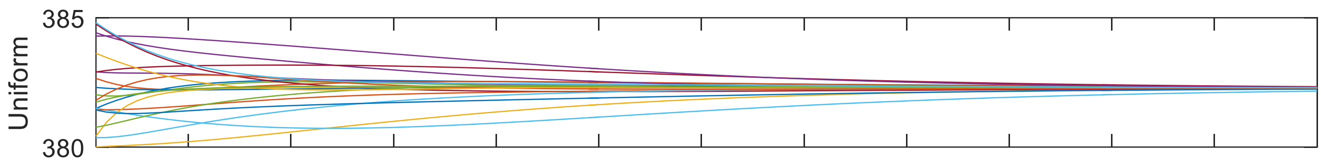	
Max-Out Degree Weight d: the maximum out-degree of the network.	$$a_{ij} = \begin{cases} \frac{1}{d+1} & j \in N_i \\ 1 - \frac{\deg_{out}(v_i)}{d+1} & i = j \\ 0 & otherwise \end{cases}$$
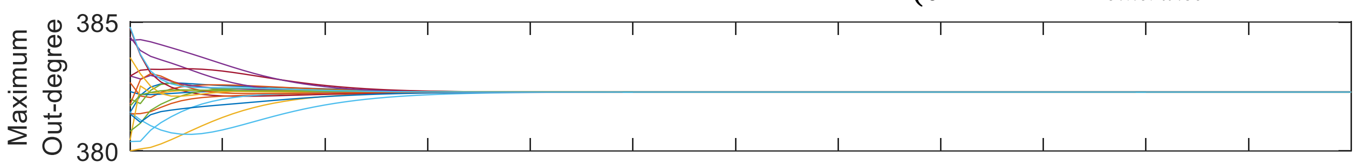	
Best Constant L: Laplacian matrix $\lambda_i(L)$: ith largest eigenvalue of L	$$a_{ij} = \begin{cases} \alpha & j \in N_i \\ 1 - \deg_{out} v_i \alpha & i = j \\ 0 & otherwise \end{cases} \quad \alpha = \frac{2}{\lambda_1(L) + \lambda_{n-1}(L)}$$
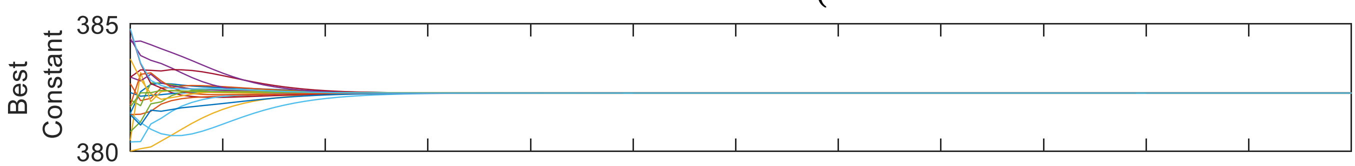	

Table 2. *Cont.*

Metropolis Weight n_i: number of neighbors of node i	$a_{ij} = \begin{cases} \frac{1}{[Max(n_i+n_j)+1]} & j \in N_i \\ 1 - \sum\limits_{j \in N_i} \frac{1}{[Max(n_i+n_j)+1]} & j = i \\ 0 & otherwise \end{cases}$

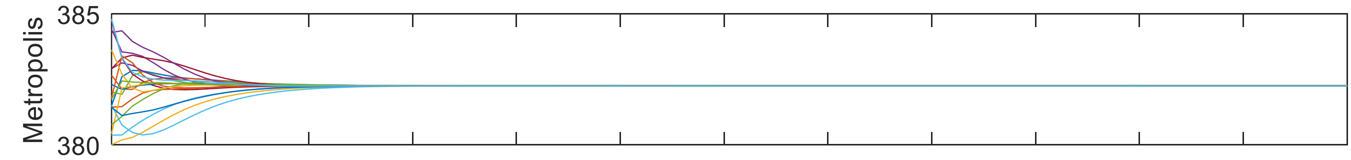

Mean Metropolis Weight ε is a very small number and for complex systems, it can be set as zero	$a_{ij} = \begin{cases} \frac{2}{(n_i+n_j+\varepsilon)} & j \in N_i \\ 1 - \sum\limits_{j \in N_i} \frac{2}{(n_i+n_j+\varepsilon)} & j = i \\ 0 & otherwise \end{cases}$

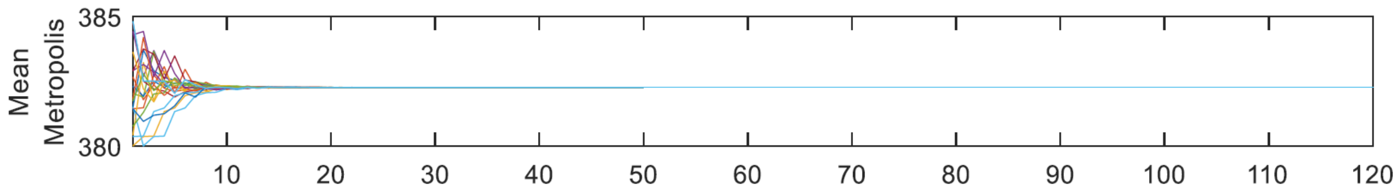

After reaching a decision on the proper updating rule and suitable network graph for the network layer of the microgrid, secondary voltage control is implemented. There are two VSI inverters in this microgrid which are responsible for final actions required for the voltage control. The network of six agents, with each agent located close to one of the critical buses, will provide the opportunity for the nodes to communicate with the neighboring nodes. The data received in each iteration will be then used to update the global consensus value according to the chosen updating rule (which is the mean metropolis weight). After reaching an agreement, the agreed average value will be used by the secondary voltage control of the VSI inverters.

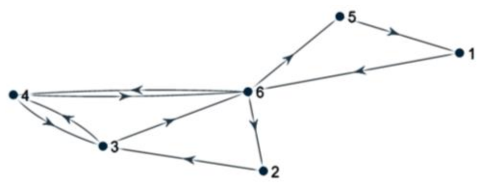

Figure 19. Network Layer of the understudied microgrid.

The secondary voltage controller is similar to a traditional droop controller with a major difference. In traditional droop-based secondary voltage control, the VSI inverter will produce active and reactive power until the VSI's local voltage is back to the predetermined setpoint. In ACA-based secondary voltage control, the set-point is not the local voltage anymore. Instead, the six nodes will agree on the average voltage of the critical buses, and this agreed average voltage value will be used for comparison with the setpoint voltage. Eventually, based on the existing error between the average voltage of critical buses, and the setpoint, proper input for the primary controllers of the VSI will be produced by a PID controller. The primary controllers will then adjust the P (real power) and Q (reactive power) being produced by these inverters. The main benefit of this method is that all critical bus voltages are taken into consideration. Any change in the load can be considered as a disturbance. This load change might be close to VSI controllers; therefore, the VSI will be able to monitor that and adapt quickly. However, if this load change happens in further-away buses, there will not be a major change in the measured voltage by VSI since traditional droop control only uses the local voltage of the VSI inverter and therefore the proper error will not be produced.

4.3. Problem Formulation

This paper compares the operation of a microgrid with and without the discussed data-driven voltage control which is based on the ACA algorithm. The first part shows the effectiveness of the proposed data-driven voltage control method using the ACA for keeping the average voltage of critical buses within desired values no matter how far the bus is from the load change. This data-driven voltage control method provides accuracy and better performance while adding to concerns related to the communication links that are the inevitable part of this data-driven control method. The second part discusses the problem that is related to the delay caused either by the communication channel or agreement process. The third part investigates the issue related to the failure of communication links due to technical malfunction or cyber-attacks [24–26].

4.3.1. Normal Operation: Decentralized vs. Data-Driven Voltage Control

There are six critical buses (nodes 1 through 6) in the test system of Figure 15. The ACA algorithm is applied to control the voltage of these six pilot buses. In a traditional decentralized voltage control, only two of these buses (the ones connected to the VSI inverters) are used to maintain their voltages at a desired level. However, in the data-driven approach, any node that is connected to the network can be considered as a pilot node, which means its voltage must remain within a certain range, even if that bus is far from the VSI inverters.

Figures 20–22 demonstrate and compare the simulation results related to traditional decentralized and ACA-based voltage control. Figure 20 depicts the average voltage of six pilot buses in the presence and absence of ACA. It is confirmed that ACA can keep the average constantly around the selected average setpoint. Figure 21 shows the voltage of each pilot bus separately for the decentralized and the ACA-based voltage control when a load change happens at bus 4. In this figure bus 4 has the lowest voltage. However, with ACA it can be better restored as the control system is trying to keep the average voltage at a proper setpoint. Finally, in Figure 22, the active and reactive power produced by each inverter are shown separately. It demonstrates the fact that PQs will work the same in both approaches but its VSI's contribution will be different.

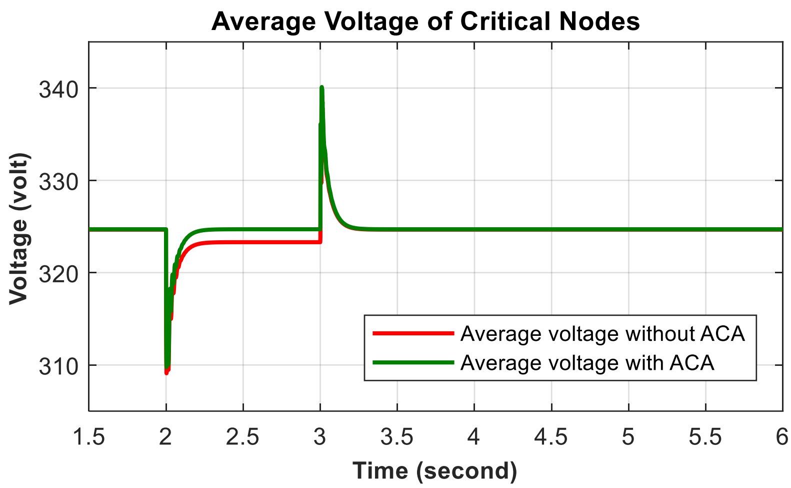

Figure 20. Average Voltage of Critical Buses with and without ACA after a Load Change at Bus 4.

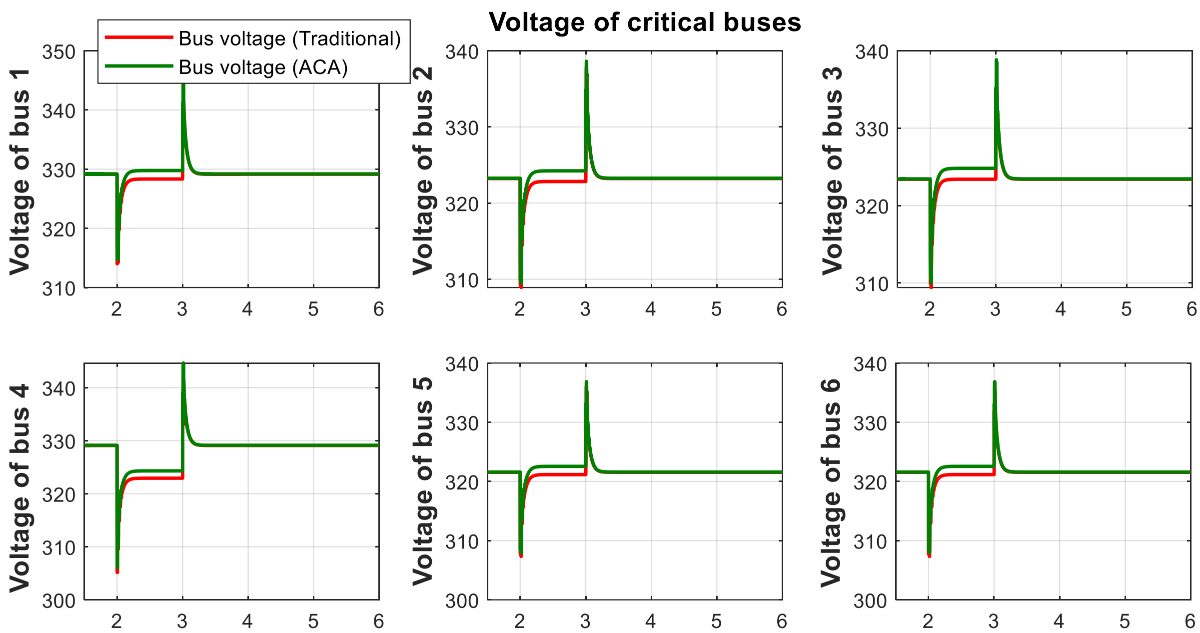

Figure 21. Voltage of Critical Buses with and without ACA after a Load Change at Bus 4.

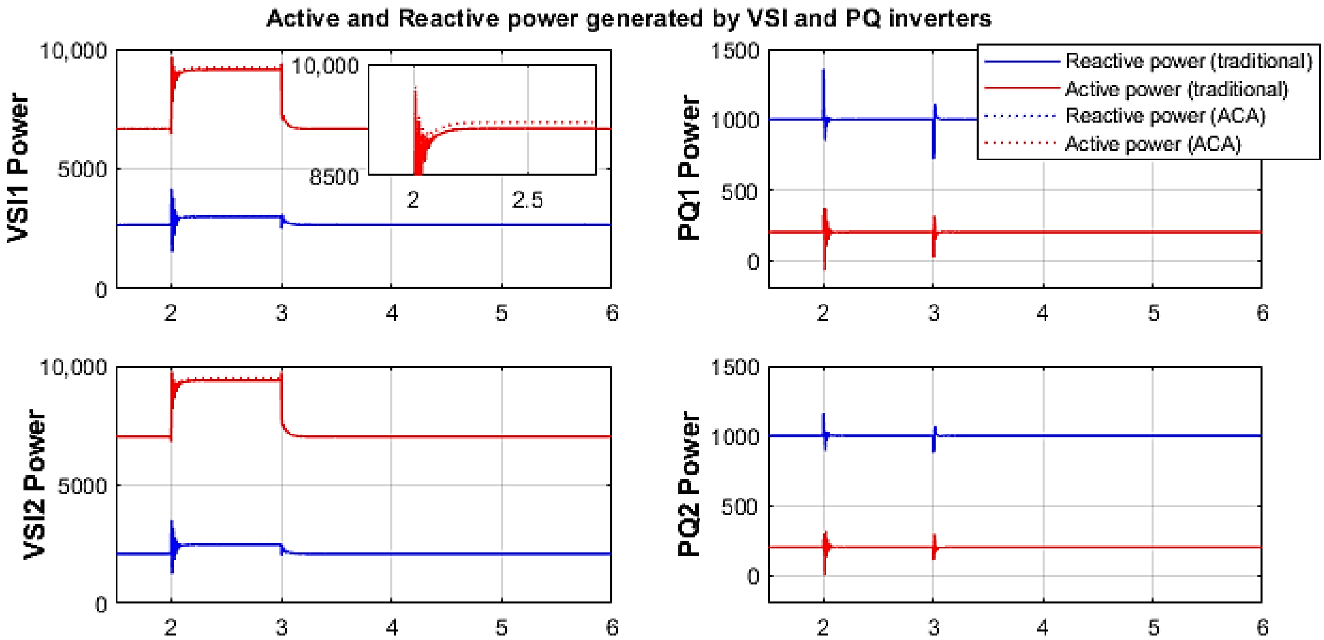

Figure 22. Active and Reactive Power Produced by Each Inverter.

4.3.2. Data-Driven Voltage Control Operation with Delay

The performance of the ACA voltage control of the microgrid is highly related to the rate of data transfer [27] and the utilized updating matrix rules to reach an agreement quickly. If there is a delay in the communication link, it can lead to oscillations in the response, and eventually, it can lead the system towards instability.

If there are communication links with high delays in the network, one approach to deal with that is to increase the connectivity factor of the system so the agreement time delay is reduced and, therefore, the overall time delay remains at the same level.

4.3.3. Data-Driven Voltage Control Operation with Communication Link Failure

Proper functionality of the ACA algorithm depends on the two previously discussed properties of the digraph of being balanced and strongly connected. If any of these two properties are violated, the required operation will not be obtained [21].

In case of a cyber-attack or a communication link failure, the balance of the digraph can be deteriorated right away. Therefore, the agreement value will not reflect the average value anymore. In a two-direction communication network, this will only affect the agreement time delay and the agreement value remains around the average value. Consequently, fault detection and isolation are sufficient. That means, in digraph, further action is required. Here are the steps to take when a one-direction communication link has a malfunction:

1. Fault detection;
2. Faulty link isolation;
3. Eliminating single or multiple non-affected one-way communication link/links to have a balanced network;
4. Adding one-way communication link if removing violates the strong connectivity.

In order to limit the impact of an attack on the adjacent nodes, the affected link and a non-affected one in the reverse direction are usually removed. However, it is essential to ensure that the communication network of the microgrid reaches an agreement so that the integrity of the microgrid's network stays strongly connected (SC). This also means that the agreement values of each node will be consistent with the average values of all nodes.

The six-node network structure of the utilized microgrid is shown in Table 3, and we illustrate how to approach a one-way link failure in order to avoid losing the correct average value. Table 3 shows the agreement process and the agreement value under different operation scenarios.

Table 3. Agreement Process and the Agreement Value under Different Operation Scenarios.

Parameters	Network Digraph	Agreement Process and the Agreement Value
Normal operation	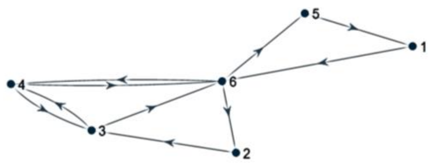	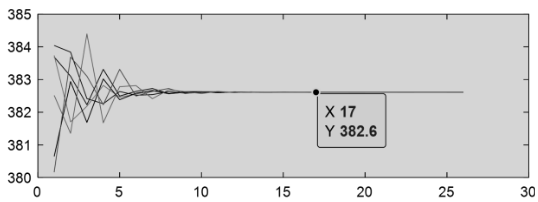
Impacted link is removed	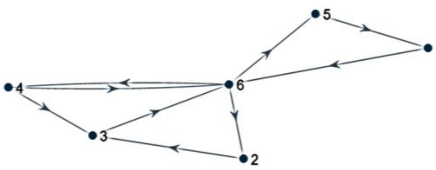	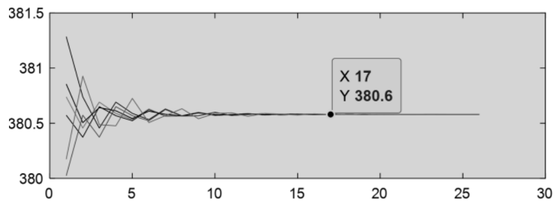
Impacted and proper non-impacted link is removed	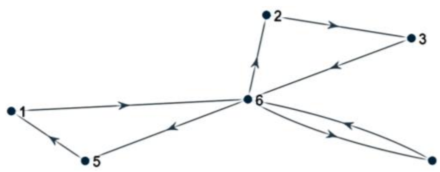	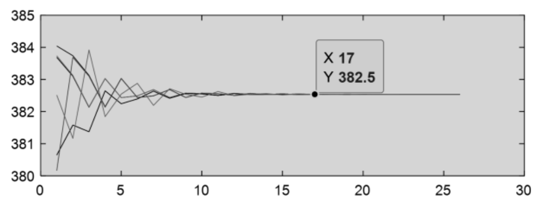

In Figure 23, the effect of both communication delays and one-way communication failure is shown and compared with normal operation. The load change is 2 + j5 kVA and it is added to bus 4 of the microgrid at t = 2 s.

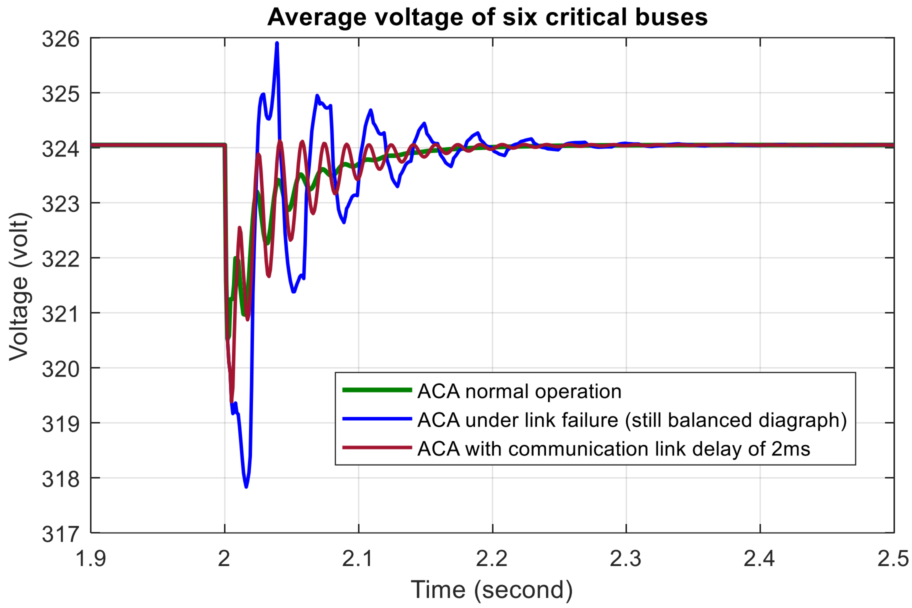

Figure 23. Average Voltage of the Pilot Buses under Different Operation Scenarios.

Figure 23 shows that the data-driven voltage control can manage the possible fragilities related to the communication structure such as delays, cyberattacks and malfunctions if proper protocols are implemented for the system to counteract the effect of malfunctions. In other words, there will be more transient response oscillation due to the delays and the link's failure, but appropriate action can ensure the required operation of the microgrid in terms of steady state response.

5. Conclusions

This paper defines an agile power system as an interconnection of flexible subsystems, including microgrids and electric vehicles, that can connect or disconnect from the main grid. This poses new challenges for their operation and control. Some of these challenges are then presented and two specific operation and control problems are addressed. The inertia provided by large generating units might not always be available. This will affect the energy balance or the load frequency control problem as well as stability. Case studies of two systems, one with two control areas and a second with three control areas, are investigated and show that the rules of interconnection are violated. It is concluded that compliance requirements set for large control areas need to be updated to account for low inertia subsystems. Finally, a data-driven voltage control approach to take advantage of the proliferation of sensors and the communication framework, which are an integral part of agile system is proposed. The data-driven secondary voltage control target is to control all critical bus voltages even if they are far from the actuators of the system (VSI inverters). Taking advantage of the computational and communicational capabilities of the network infrastructure, along with the proposed Average Consensus Algorithm (ACA)-based secondary voltage control, all critical bus voltages can be kept in their desired range. Additionally, the possible fragilities of the communication structure such as delays, cyberattacks and malfunctions are addressed for the proposed data-driven voltage control of microgrids.

Future work will address the effect of low inertia on the dynamic stability of agile systems and the appropriate design of controllers to improve the performance. Another problem might be to solve the economic dispatch through interactions of the power system and the electric transportation system.

Author Contributions: Conceptualization, A.F. and F.D.M.; methodology, A.F., F.D.M. and H.K.V.; software, A.F., F.D.M. and H.K.V.; validation, A.F. and H.K.V.; formal analysis, A.F.; investigation, F.D.M.; resources, H.K.V.; data curation, A.F. and F.D.M.; writing—original draft preparation, A.F. and F.D.M.; writing—review and editing, A.F. and H.K.V.; visualization, A.F.; supervision, A.F.; project administration, A.F.; funding acquisition, A.F. All authors have read and agreed to the published version of the manuscript.

Funding: This research received no external funding.

Conflicts of Interest: The authors declare no conflict of interest.

References

1. EPRI White Paper. *Electric Power System Flexibility: Challenges and Opportunities*; Electric Power Research Institute: Palo Alto, CA, USA, 2016.
2. Syed, M.H.; Guillo-Sansano, E.; Mehrizi-Sani, A.; Burt, G.M. Load Frequency Control in Variable Inertia Systems. *IEEE Trans. Power Syst.* **2020**, *35*, 4904–4907. [CrossRef]
3. Michael, D. A Road Test for Vehicle-to-Grid Tech. *IEEE Spectrum* **2022**, *59*, 20–25.
4. Salem, A. *Internet of Things in Smart Grids*; MS Project; West Virginia University: Morgantown, WV, USA, 2015.
5. Peck, M.E.; Wagman, D. Energy trading for fun and profit buy your neighbor's rooftop solar power or sell your own-it'll all be on a blockchain. *IEEE Spectrum* **2017**, *54*, 56–61. [CrossRef]
6. Available online: https://seekingalpha.com/article/4262588-californias-mid-day-solar-power-glut-become-obvious (accessed on 8 October 2022).
7. Available online: https://ics.sans.org/media/E-ISAC_SANS_Ukraine_DUC_5.pdf (accessed on 8 October 2022).
8. Available online: http://www.caiso.com/TodaysOutlook/Pages/index.html (accessed on 8 October 2022).
9. Mohammadi, F.D.; Vanashi, H.K.; Feliachi, A. State Space Modeling, Analysis and Distributed Secondary Frequency Control of Isolated Microgrids. *IEEE Trans. Energy Convers.* **2018**, *33*, 155–165. [CrossRef]
10. Mohammadi, F.D.; Keshtkar, H.; Banadaki, A.D.; Feliachi, A. A novel cooperative distributed secondary controller for VSI and PQ inverters of AC microgrids. *Heliyon* **2019**, *5*, e01823. [CrossRef] [PubMed]
11. Shahirina, A.H.; Hajizadeh, A.; Yu, D.C.; Feliachi, A. Control of a Hybrid Wind Turbine/Battery Energy Storage Power Generation System Considering Statistical Wind Characteristics. *J. Renew. Sustain. Energy* **2012**, *4*, 17. [CrossRef]
12. Ghorbani, M.J.; Choudhry, M.A.; Feliachi, A. A Multi-Agent Design for Power Distribution Systems Automation. *IEEE Trans. Smart Grids* **2016**, *7*, 329–339. [CrossRef]
13. Hajizadeh, A.; Feliachi, A.; Golkar, M.A. Intelligent Power Management of a Hybrid Fuel Cell/Energy Storage Distributed Generator. *Smart Power Grid* **2011**, *8*, 265–285.
14. Feliachi, A.; Belkacemi, R. Intelligent Multi-agent System for Smart Grid Power Management. *Smart Power Grid* **2011**, *16*, 515–542.
15. Available online: https://www.cleanenergyreviews.info/blog/2014/5/4/how-solar-works (accessed on 8 October 2022).
16. Available online: https://www.nerc.com/pa/comp/Pages/default.aspx (accessed on 8 October 2022).
17. Beddard, G.; Stanisha, E.; Mohammadi, F.D.; Keshtkar, H. Effect of Cyber Attacks on the Performance of Optimally Designed Network for Distributed Secondary Voltage Control in Microgrids. In *Proceedings of the Future Technologies Conference (FTC)*; Arai, K., Ed.; Springer: Cham, Switzerland, 2021; Volume 3.
18. Keshtkar, H.; Mohammadi, F.D.; Ghorbani, J.; Solanki, J.; Feliachi, A. Proposing an improved optimal LQR controller for frequency regulation of a smart microgrid in case of cyber intrusions. In Proceedings of the 2014 IEEE 27th Canadian Conference on Electrical and Computer, Engineering (CCECE), Toronto, Canada, 4–7 May 2014; pp. 1–6.
19. Zuo, S.; Beg, O.A.; Davoudi, A.; Lewis, F.L. Resilient Networked AC Microgrids Under Unbounded Cyber Attacks. *IEEE Trans. Smart Grid* **2020**, *11*, 3785–3794. [CrossRef]
20. Olfati-Saber, R.; Murray, R.M. Consensus problems in networks of agents with switching topology and time-delays. in Automatic Control. *IEEE Trans. Autom. Control.* **2004**, *49*, 1520–1533. [CrossRef]
21. Mohammadi, F.D.; Keshtkar, H.; Feliachi, A. Optimum Communication Network Design for Distributed Secondary Voltage Control in Microgrids. In Proceedings of the 2019 IEEE PowerTech, Milan, Italy, 23–27 June 2019; pp. 1–6.
22. Liu, W.; Gu, W. Decentralized Multi-Agent system-Based cooperative Frequency Control for Autonomous Microgrids with Communication Constraints. *IEEE Trans. Sustain. Energy* **2014**, *5*, 446–456. [CrossRef]
23. Xu, Y.; Liu, W. Novel Multiagent Based Load Restoration Algorithm for Microgrids. *IEEE Trans. Smart Grid* **2011**, *2*, 152–161. [CrossRef]
24. Wood, A.J.; Wollenberg, B.F.; Sheblé, G.B. *Power Generation, Operation and Control*, 3rd ed.; John Wiley & Sons: Hoboken, NJ, USA, 2014.
25. Li, T.; Peng, G.; Zhu, Q.; Başar, T. The Confluence of Networks, Games, and Learning a Game-Theoretic Framework for Multiagent Decision Making Over Networks. *IEEE Control Syst. Mag.* **2022**, *42*, 35–67. [CrossRef]

26. Hu, G.; Pang, Y.; Sun, C.; Hong, Y. Distributed Nash Equilibrium Seeking: Continuous-Time Control-Theoretic Approaches. *IEEE Control Syst. Mag.* **2022**, *42*, 68–86. [CrossRef]
27. Mohammadi, F.D.; Keshtkar, H.; Feliachi, A.; Kulathumani, V. Design of an adaptive sending rate for frequency regulation of a smart microgrid with optimal LQR controller. In Proceedings of the 2017 IEEE Power & Energy Society Innovative Smart Grid Technologies Conference (ISGT), Washington, DC, USA, 23–26 April 2017; pp. 1–5.